Original Research *Feature article*

A metabolism-relevant signature as a predictor for prognosis and therapeutic response in pancreatic cancer

Qiangda Chen[1,2,*], Ning Pu[1,2,*], Hanlin Yin[1,2,*], Jicheng Zhang[1,2], Guochao Zhao[1,2], Wenhui Lou[1,2] and Wenchuan Wu[1,2]

[1]Department of General Surgery, Zhongshan Hospital, Fudan University, Shanghai 200032, China; [2]Cancer Center, Zhongshan Hospital, Fudan University, Shanghai 200032, China

Corresponding authors: Wenchuan Wu. Email: wuwenchuan1973@126.com; Wenhui Lou. Email: louzsh@126.com

*These authors contributed equally to this work.

Impact statement

Pancreatic cancer (PC) is characterized by an extremely poor prognosis and limited curative effect. Metabolic reprogramming, which emerged as one of the novel hallmarks of cancers, has been identified as a key regulator of tumorigenesis in PC. Therefore, we attempted to establish a metabolic signature to predict the prognosis and chemotherapy response. Our results revealed that a five-gene metabolic signature was a potential novel prognostic and therapeutic biomarker for optimizing individualized treatment for PC patients.

Abstract

Although several altered metabolic genes have been identified to be involved in the tumorigenesis and advance of pancreatic cancer (PC), their prognostic values remained unclear. The purpose of this study was to explore new targets and establish a metabolic signature to predict prognosis and chemotherapy response for optimal individualized treatment. The expression data of PC patients from two independent cohorts and metabolism-related genes from KEGG were utilized and analyzed for the establishment of the signature via lasso regression. Then, the differentially expressed candidate genes were further confirmed via online data mining platform and qRT-PCR of clinical specimens. Then, the analyses of gene set enrichment, mutation, and chemotherapeutic response were performed via R package. As results showed, 109 differentially expressed metabolic genes were screened out in PC. Then a metabolism-related five-gene signature comprising B3GNT3, BCAT1, KYNU, LDHA, and TYMS was constructed and showed excellent ability for predicting survival. A novel nomogram coordinating the metabolic signature and other independent prognostic parameters was developed and showed better predictive power in predicting survival. In addition, this metabolic signature was significantly involved in the activation of multiple oncological pathways and regulation of the tumor immune microenvironment. The patients with high risk scores had higher tumor mutation burdens and were prone to be more sensitive to chemotherapy. In summary, our work identified a new metabolic signature and established a superior prognostic nomogram which may supply more indications to explore novel strategies for diagnosis and treatment.

Keywords: Pancreatic cancer, metabolic signature, prediction, prognosis, chemotherapeutic response

***Experimental Biology and Medicine* 2022; 247: 120–130. DOI: 10.1177/15353702211049220**

Introduction

Pancreatic cancer (PC) is a deadly malignancy with a five-year overall survival (OS) rate of approximately 10%.[1] In the past decades, the advances in multiple therapeutic strategies, such as targeted therapies[2] and immunotherapy,[3,4] have made relevant but limited progress in outcomes partly due to PC's complexity and heterogeneity. It is quite necessary to put personalized systemic therapy into practice. Thus, an accurate predictive model for PC to assess the treatment efficacy and survival outcomes will be valuable. With the advances of transcriptome sequencing, traditional parameters incorporated with prognosis-related gene signatures have shown more robust power in survival prediction for PC patients.

Metabolic reprogramming has regained widespread attention over the past decade.[5] Recently, increasing studies have indicated that the alterations of specific metabolic pathways in PC could contribute to tumor growth, therapeutic resistance, and immune escape.[6,7] For example, CD73, a cell surface protein overexpressed in PC, could

reduce the infiltrating $CD8^+$ T cells in tumor to promote immune escape.[8] Intriguingly, some oncogenes and antioncogenes like KRAS and TP53 have also been proved to support tumor growth by rewiring metabolism.[9] Moreover, alterations in glutamine metabolism have been found to participate in PC progression in human cell lines and animal models.[10] Thus, some promising therapeutic targets may emerge under aberrant metabolism in PC. However, the role of these metabolic genes in PC remained unclear. Therefore, it is necessary to explore a metabolism-related gene signature to realize individualized predictions for outcome and treatment response.

In this study, we integrated TCGA and GEO databases to discover differentially expressed metabolic genes (DEMGs). Prognostic DEMGs were identified by univariate and Lasso-Cox regression analyses. Next, a metabolism-related signature was proposed and validated in two independent datasets respectively. Additionally, the potential molecular mechanism, immune cell infiltrating pattern, tumor mutation burden (TMB), and chemotherapy response related to the formulated signature were also investigated.

Materials and methods

Data collection

The normalized gene expression data, somatic mutation data, and relevant clinicopathologic information were obtained from the UCSC Xena and GEO. The TCGA cohort includes 178 PC samples and only 4 normal pancreatic tissue samples, so 167 normal pancreatic tissue samples from the Genotype-Tissue Expression (GTEx) were developed as the supplement of the TCGA dataset. The gene expression microarray dataset GSE62452 included 61 normal pancreatic tissue samples and 69 PC samples. However, 10 cases were excluded because of a follow-up period <30 days or insufficient TNM stage in the TCGA cohort. Among the 69 PC patients in GEO cohort, 4 cases were excluded as the survival time was unknown. Finally, 168 cases with complete clinical information in TCGA cohort, including gender, age, race, grade, AJCC_M, AJCC_N, AJCC_T, stage, family history, chronic pancreatitis, diabetes history, chemotherapy, neoadjuvant treatment, radiation therapy, alcohol history and tumor site, and 65 samples from the GEO dataset were enrolled.

Recognition of DEMGs

The Limma package in R was applied to recognize the differentially expressed genes between tumors and normal samples in TCGA plus GTEx dataset and GEO dataset. The cutoff value of $\log_2$FC was 0.5, and the *P* value was 0.05. Metabolic genes that participated in metabolic pathways according to KEGG pathway gene sets from MSigDB database were extracted from the previous research.[11] The overlap of genes among the above three gene lists was retained as DEMGs.

Bioinformatic DEMGs analysis

The potential biological functions of DEMGs were investigated via GO and KEGG analyses. The protein–protein interaction (PPI) network of DEMGs was built by STRING.[12] Then, the interacting data derived from STRING was input to Cytoscape3.7.2. The cytoHubba, a Cytoscape plugin, was utilized to explore hub nodes via maximal clique centrality (MCC) method.

Development and validation of the metabolic signature

Univariate Cox regression was used to assess the prognostic role of DEMGs, and the *P* value <0.01 was set as statistical significance. Next, the Lasso-Cox regression via survival and glmnet package was applied to delete highly related genes and avoid over-fitting. Then, the rest genes of DMEGs were further evaluated by stepwise multivariate Cox regression analysis. Finally, the metabolic signature was established. Then, the patients were divided into two groups according to the optimal cut-off value. Further, receiver operating characteristic (ROC) curve analysis and Kaplan-Meier analysis were performed to compare the survival outcome and predictive power.

Collection of clinical samples

Twenty-five pairs of PC and paracancer samples were got from patients with histologically diagnosed pancreatic ductal adenocarcinoma after R0 radical surgery from January to May 2019 in Zhongshan Hospital, Fudan University. All patients with distal metastasis, history of malignant cancer, or hematological system diseases were excluded from our cohort. All samples were stored at –80°C as soon as possible. The informed consent was signed by all patients and the protocol was permitted by the ethical committee of Zhongshan Hospital, Fudan University.

External validation of the mRNA and protein levels of the five metabolic genes

Oncomine was applied to validate the mRNA level of the candidate genes in the gene signature.[13] The total RNAs of 25 pairs of t tissues were obtained by TRIzol Reagent. Then, reverse transcription and qRT-PCR were performed as our previous report.[14] The qPCR data were normalized to ACTB using the $-\Delta\Delta$Ct method. The primer sequences are summarized in Table S1. Finally, the differential protein levels of these candidate genes were further validated in the Human Protein Atlas database (HPA).[15]

Construction of a predictive nomogram

The independent prognostic factors were recognized via univariate and multivariate Cox regression analyses and then based on which a novel prognostic nomogram was formulated by rms package. The classification efficiency of the prognostic model was further estimated via Kaplan-Meier analysis, ROC analysis, and calibration plot. Finally, the clinical value of this nomogram was assessed via decision curve analysis (DCA).

Gene set enrichment analyses

Gene set enrichment analysis (GSEA)[16] was performed to explore differential gene sets enriched in high- and low-risk groups. The selected gene sets were c2.cp.kegg, c5.go.bp, cc, mf, and h.all.v.7.0.symbols. The gene set was significantly enriched, with a false discovery rate <0.05.

Analysis of tumor microenvironment

ESTIMATE,[17] a widely used algorithm, was applied to estimate the tumor purity, infiltrating immune, and stroma cells via analysis of normalized gene expression profiles. Furthermore, CIBERSORT, an analytic algorithm,[18] was used to evaluate the infiltration of 22 immune cell types.

Tumor mutation analysis

TMB was evaluated by the calculation of tumor-specific mutation genes. TMB levels were visualized and compared via "maftools" package in the TCGA cohort. Moreover, the correlation between risk scores and TMB was further evaluated.

Evaluation of the responses to chemotherapeutic agents

The "pRRophetic" package was used to predict the response of chemotherapeutic agents for PC patients based on the TCGA gene expression profiles.[19]

Statistical analysis

R software (version 3.6.3) was applied to conduct all statistical analyses in this study. Unless otherwise stipulated, the P value <0.05 was considered statistically significant.

Results

Identification of DEMGs

The flow chart outlines how this study was performed (Figure S1). The DEGs were initially analyzed using the high-throughput gene expression data of the TCGA plus GTEx and the GSE62452 cohort; 11452 and 1482 DEGs were found in the TCGA plus GTEx and the GSE62452. Then, 1466 metabolism-related genes were obtained as the previous report.[11] Finally, 109 DEMGs were obtained by the overlap of the above three lists (Figure 1(a)).

PPI network and functional enrichment analysis of DEMGs

To analyze the gene interactions of DEMGs, a PPI network that contained 400 interactions and 104 nodes was established by STRING. Then, the hub genes that scored in the top 10 by the MCC method were obtained (Figure 1(b)), which might be potentially promising targets for PC.

To investigate the biological function of 109 DEMGs in PC, GO and KEGG analyses were conducted. The DEMGs mainly participated in the process of organic acid biosynthesis and small molecule catabolism via GO analysis (Figure 1(c)). KEGG analysis showed that DEMGs were enriched in pathways associated with glycolysis, carbon biosynthesis, and metabolism (Figure 1(d)).

Establishment and validation of a metabolic gene signature for predicting prognosis

First, 13 survival-related DEMGs were identified through the univariate Cox regression analysis (Figure 2(a)). Then, Lasso regression was conducted to delete highly related genes and avoid over-fitting (Figure S2). Next, UDP-GlcNAc:BetaGal Beta-1,3-N-Acetylglucosaminyltransferase 3 (B3GNT3), branched-chain amino acid transaminase 1 (BCAT1), kynureninase (KYNU), lactate dehydrogenase A (LDHA), and thymidylate synthetase (TYMS) were stepwise confirmed as independent prognostic genes through multivariate Cox analysis (Figure 2(b)). Then, a 5-gene signature was established. Risk score $= 0.2805 \times \text{Exp}$ B3GNT3 $+ 0.3705 \times \text{Exp}$ BCAT1 $+ 0.4273 \times \text{Exp}$ KYNU $+ 0.3774 \times \text{Exp}$ LDHA $+ 0.5490 \times \text{Exp}$ TYMS. Overall information about these five genes was summarized in Table 1. Patients were separated into two groups according to the optimal cutoff for risk score (Figure S3a). The median OS for the patients was 12.0 and 15.8 months in high- and low-risk group, respectively, which revealed a marked difference in prognosis ($P < 0.001$, Figure 2(c)). The area under the ROC curves (AUCs) were 0.768, 0.712, and 0.730 for 1-, 2-, and 3-year OS (Figure 2(e)).

Then, the external dataset GSE62452 was applied to confirm the prognostic performance of this signature. The grouping method was the same as for the TCGA cohort (Figure S3b). The median OS in high-risk and low-risk group was 9.6 and 21.2 months. Furthermore, the patients in high-risk group had a worse outcome than those in low-risk group ($P < 0.001$, Figure 2(d)). The AUCs were 0.677, 0.731, and 0.795 for 1-, 2-, and 3-year OS (Figure 2(f)). Collectively, the formulated metabolic signature showed a superior ability at evaluating OS of PC.

Evaluation of independent prognostic factors

To investigate independent prognostic factors, 168 patients with comprehensive clinicopathologic information in TCGA cohort were included. Univariate and multivariate analyses were conducted to assess the relationships between these indicators and survival. We found that age, grade, AJCC_N, AJCC_T, chemotherapy, and risk score were related to OS in the univariate analysis (Figure 3(a)). Furthermore, age, chemotherapy, and risk score were further perceived as remarkable independent prognostic indicators by multivariate analysis (Figure 3(b)).

Building a novel predictive nomogram with the TCGA-PAAD cohort

The patients with comprehensive clinicopathologic data in the TCGA cohort were enrolled to establish the nomogram predicting 1-, 2-, and 3-year OS via stepwise Cox regression. The age, AJCC_N, chemotherapy, and risk score were incorporated into the nomogram (Figure 4(a)). The AUCs were 0.764, 0.843, and 0.863 for 1-, 2-, and 3-year OS (Figure 4(b)). Meanwhile, patients were separated into

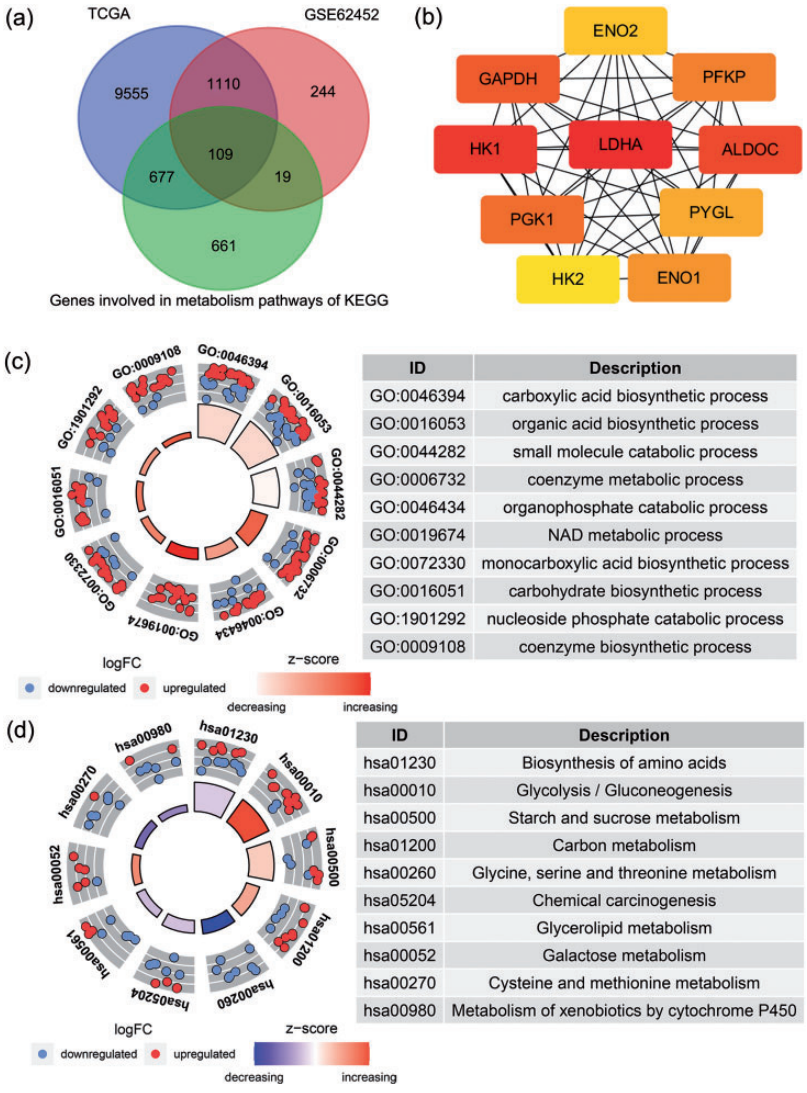

ID	Description
GO:0046394	carboxylic acid biosynthetic process
GO:0016053	organic acid biosynthetic process
GO:0044282	small molecule catabolic process
GO:0006732	coenzyme metabolic process
GO:0046434	organophosphate catabolic process
GO:0019674	NAD metabolic process
GO:0072330	monocarboxylic acid biosynthetic process
GO:0016051	carbohydrate biosynthetic process
GO:1901292	nucleoside phosphate catabolic process
GO:0009108	coenzyme biosynthetic process

ID	Description
hsa01230	Biosynthesis of amino acids
hsa00010	Glycolysis / Gluconeogenesis
hsa00500	Starch and sucrose metabolism
hsa01200	Carbon metabolism
hsa00260	Glycine, serine and threonine metabolism
hsa05204	Chemical carcinogenesis
hsa00561	Glycerolipid metabolism
hsa00052	Galactose metabolism
hsa00270	Cysteine and methionine metabolism
hsa00980	Metabolism of xenobiotics by cytochrome P450

Figure 1. Identification and functional enrichment analysis of the DEMGs. (a) Venn diagram of the DEMGs intersected in TCGA, GEO, and KEGG metabolism pathway datasets. (b) Visualization of top 10 hub genes identified by Cytoscape. (c) Top 10 enriched biological processes of the DEMGs (d) Top 10 enriched KEGG pathway of the DEMGs. DEMGs, differentially expressed metabolic genes. (A color version of this figure is available in the online journal.)

two groups based on the optimal cutoffs of this nomogram. Those patients with higher risk had markedly worse OS ($P < 0.001$, Figure 4(c)). Moreover, the calibration plots displayed good agreement with the actual observed values and the established nomogram could bring more net benefit for predicting survival than single factor via the DCA curves (Figure S4a-b), which further confirmed the predictive ability of our nomogram and might support more clinical management.

External validation of differential expression of target genes

Differential expression levels of the targeted genes were validated via Oncomine. B3GNT3, KYNU, LDHA, and TYMS were found to be significantly increased, while BCAT1 was markedly decreased in PC (Figure S5), which was consistent with the qRT-PCR results of tissues from our center (Figure 5(a)). Table S2 outlines the clinicopathological features of the patients. Meanwhile, their protein levels were explored by HPA. Typical images of immunohistochemistry of five genes in cancer and paracancer tissues are displayed in Figure 5(b). Taking together, these results further confirmed the associations between these five genes and PC occurrence to some extent.

Gene signature related pathway analysis

To explore the biological features of this metabolic signature, GSEA was performed. Pathways included glycolysis, G2M checkpoint, mTORC1 signaling, hypoxia, cell cycle, pyrimidine metabolism, nucleotide excision repair, and DNA replication were enriched in high-risk group via Hallmark and KEGG analysis (Figure S6a). Meanwhile, GO analysis also displayed that molecular alterations in the high-risk group might contribute to the malignant behaviors of PC, particularly proliferation (Figure S6b).

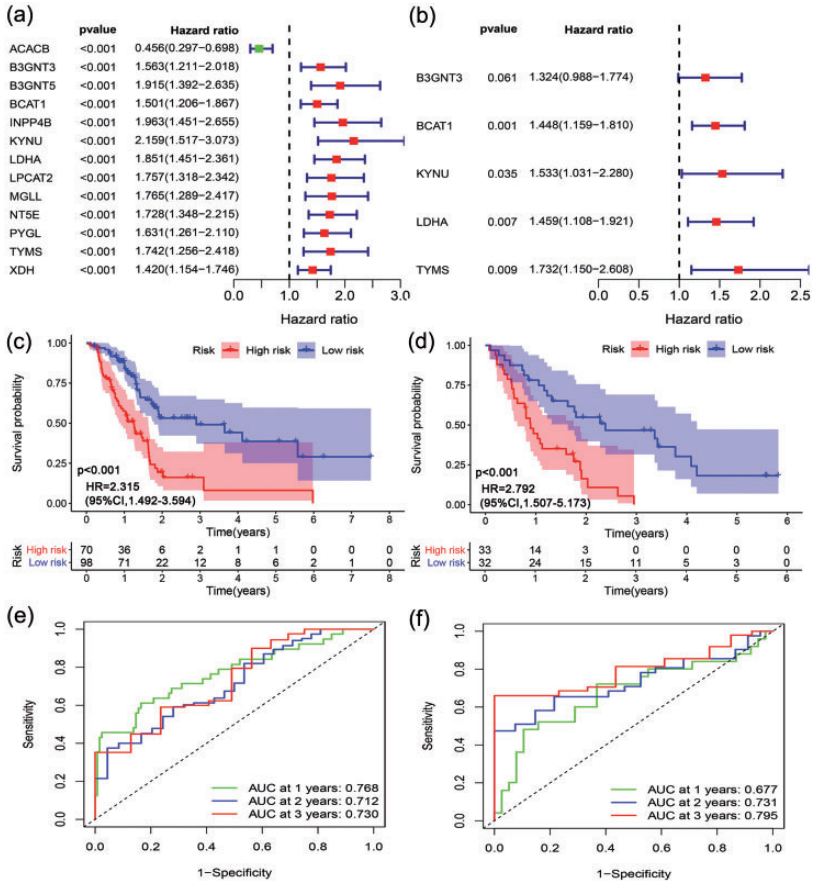

Figure 2. Construction and validation of metabolic signature. (a) Forest plot of the 13 significant MDEGs ($P < 0.001$) identified by the univariate Cox regression. (b) Forest plot of the five significant MDEGs recognized by Lasso-cox regression. (c) The Kaplan-Meier plot for OS in TCGA cohort. (d) The Kaplan-Meier plot for OS in GEO cohort. (e) Time-independent ROC curves of the metabolic signature in TCGA cohort. (f) Time-independent ROC curves of the metabolic signature in GEO cohort. OS, overall survival. (A color version of this figure is available in the online journal.)

Table 1. Overall information of five genes constructing the prognostic signature.

Gene	Gene full name	Location	Hazard ratio	Coefficient
B3GNT3	UDP-GlcNAc:BetaGal Beta-1,3-N-Acetylglucosaminyltransferase 3	chr19:17,794,828-17,813,576	1.324	0.28
BCAT1	Branched Chain Amino Acid Transaminase 1	chr12:24,810,024-24,949,101	1.448	0.371
KYNU	Kynureninase	chr2:142,877,657-143,055,833	1.533	0.427
LDHA	Lactate Dehydrogenase A	chr11:18,394,389-18,408,425	1.459	0.377
TYMS	Thymidylate Synthetase	chr18:657,653-673,578	1.732	0.549

Associations between the infiltrating immune cells and risk score

Since interruption of some metabolic pathways may influence the chemotaxis and activation of immune cells to modulate immunity, the association between risk score and the infiltration of immune/stromal cells and tumor purity was evaluated. Based on the transcriptomic data from TCGA cohort, the immune-, stromal-, and estimate scores were calculated via ESTIMATE algorithm. The immune scores and estimate scores were lower in high-risk group, suggesting that fewer infiltrating immune cells and higher tumor purity ($P < 0.05$, Figure 6(a)). Additionally, the infiltration levels of the 22 immune cells were further evaluated in TCGA cohort (Figure S7a). The high-risk group had lower infiltration levels of naïve B cells, $CD8^+$ T cells, and monocytes, while the proportions of activated dendritic cells, M0 macrophages, and activated memory $CD4^+$ T cells were relatively higher ($p < 0.05$, Figure 6(b)). Likewise, the landscape of tumor-infiltrating immune cells based on the transcriptomic data from the GSE62165 cohort was further estimated to avoid bias from a single dataset (Figure S7b). The proportions of resting mast cells, activated NK cells $CD8^+$ T cells, and monocytes were lower in high-risk group, whereas the infiltrations of resting dendritic cells, eosinophils, and M0 macrophages were comparatively higher ($P < 0.05$, Figure S7c). $CD8^+$ T cells, monocytes, and M0 macrophages were significantly altered in both datasets. Then, Figure 6(c) showed that the expression levels of mostly immunomodulatory molecules were relatively lower in high-risk group, further

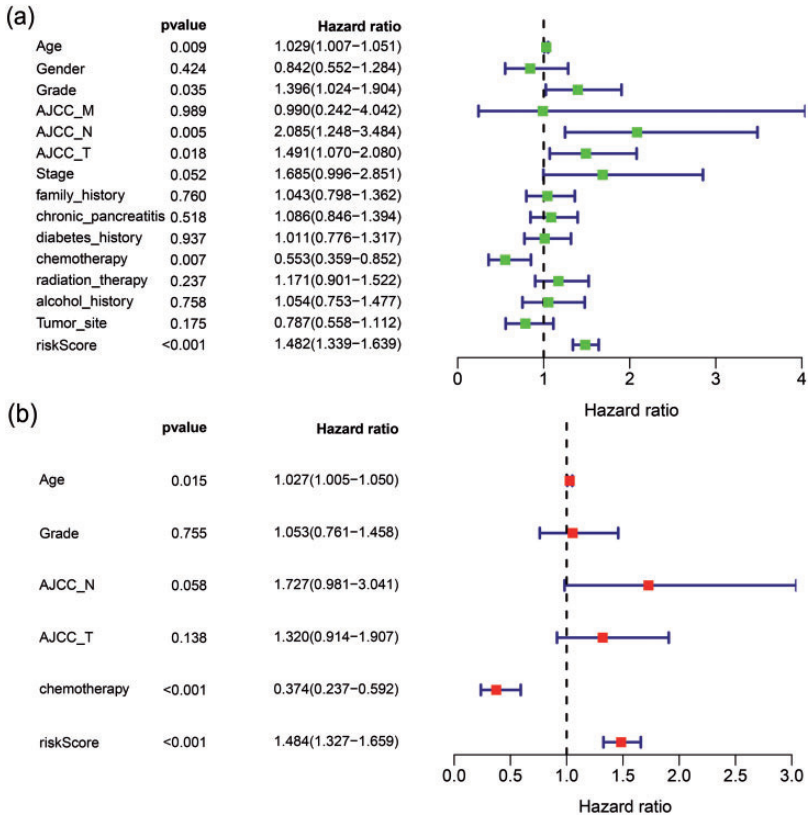

Figure 3. Cox regression analysis of independent prognostic factors in PC. (a) Forest plot of the prognostic factors identified by univariate Cox regression. (b) Forest plot of independent factors identified by multivariate Cox regression. PC, pancreatic cancer. (A color version of this figure is available in the online journal.)

supporting that the microenvironment in the high-risk group was prone to be immunologically "cold."

Analysis of tumor mutation burden

The mutation of relevant oncogenes and tumor suppressor genes in PC could rewire metabolism to support tumor growth.[9] Thus, the association between this metabolic signature and TMB was further investigated. The gene-altered landscapes in PC are displayed in Figure S8a-b. Five genes were mutated in ≥10% of patients within low-risk group: KRAS (64%), TP53 (58%), TTN (20%), SAMD4 (19%), and CDKN2A (13%). Six genes were mutated in ≥10% of patients within the high-risk group: KRAS (93%), TP53 (75%), SMAD4 (28%), CDKN2A (22%), FLG (10%), and RNF43 (10%). Especially, the rates of KRAS and TP53 mutation were relatively higher, whereas the rate of TTN was comparatively lower in the high-risk group ($P < 0.05$). Meanwhile, higher TMB was found in patients with high-risk scores ($P = 0.01$, Figure S9a), and its positive correlation was further confirmed ($P < 0.001$, Figure S9b). Therefore, the mutation of the oncogenes and antioncogenes might promote metabolic reprogramming in PC.

Responses to chemotherapy

As adjuvant strategies develop, chemoresistance remains the major obstacle in PC treatment. Accumulative evidence indicated that specific metabolic aberrations of PC cells were associated with chemoresistance.[21] Therefore, the ability of risk score in predicting the chemotherapy response was further estimated with the pRRophetic algorithm. The IC50 of four common chemotherapeutic agents used in PC was predicted. Paclitaxel, Cisplatin, and Erlotinib except for Gemcitabine have lower IC50 in the high-risk group ($P < 0.05$), indicating these patients with higher risk scores were more sensitive to these three drugs (Figure 7(a)). Then, the ability of the constructed signature in predicting the prognosis of patients with or without chemotherapy was separately assessed in high-risk group; the prognosis of patients without chemotherapy was comparatively poorer than those with chemotherapy (Figure 7(b)). However, no obvious differences in prognosis between patients with chemotherapy or not were observed in low-risk group (Figure 7(c)). Such a metabolic gene signature remained to be accurate in predicting response to chemotherapy.

Discussion

PC is a deadly malignant tumor with an extremely poor prognosis.[1] While great achievements about therapeutic strategies have been made to improve the prognosis, the effects remain to be limited. The patients who possessed similar clinicopathological parameters such as TNM staging could have totally different outcomes. Prediction of prognosis and identification of tumor heterogeneity are needed to be more accurate to administrate individual treatment. The progress of sequencing technology has promoted the establishment of novel predictive tools based on

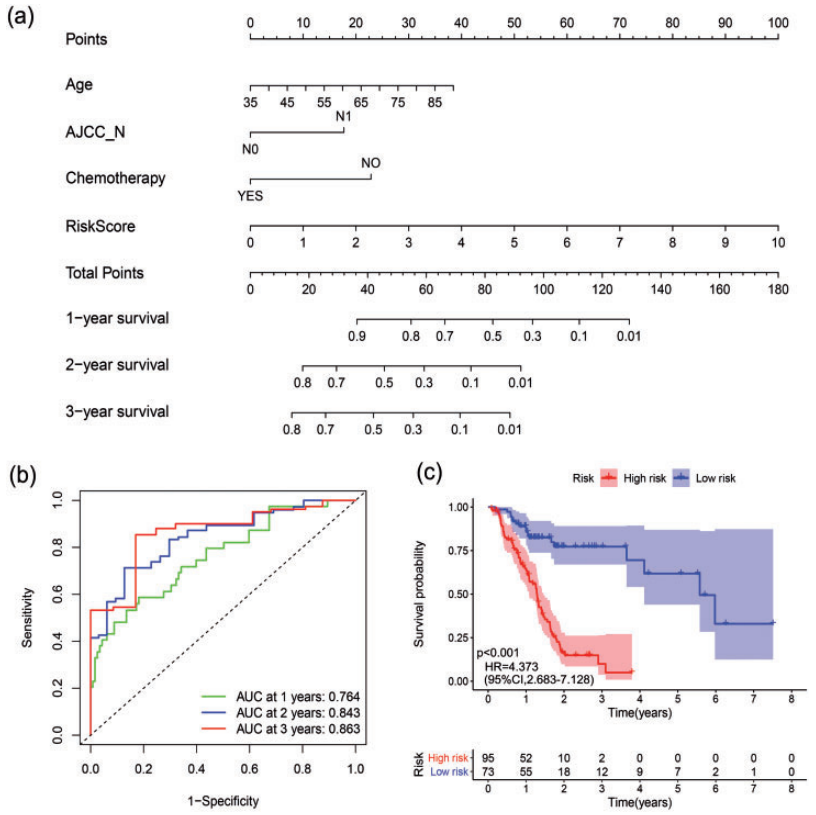

Figure 4. Prognostic nomogram for predicting overall survival of PC patients. (a) A prognostic nomogram was developed by combining clinicopathologic factors with the gene signature in PC. (b) Time-independent ROC curves of the nomogram. (c) Kaplan-Meier curves of the nomogram. The patients were stratified based on the median for the nomogram. PC, pancreatic cancer. (A color version of this figure is available in the online journal.)

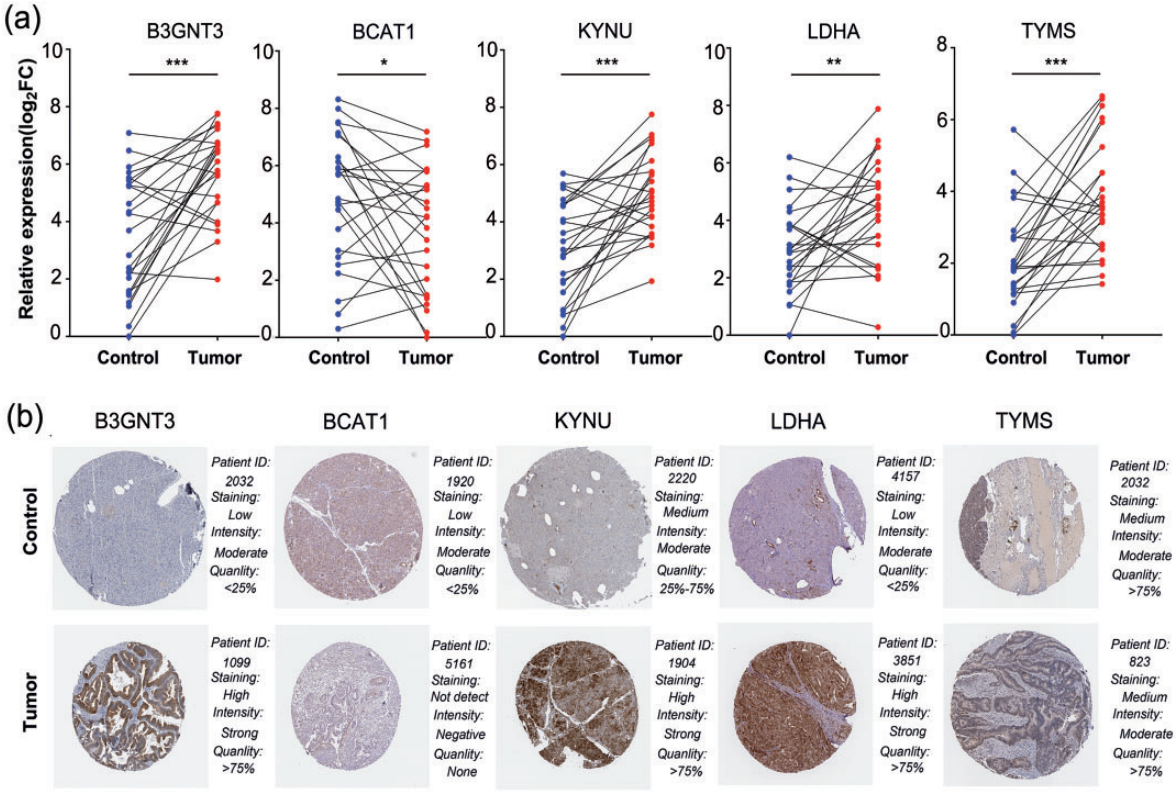

Figure 5. External validation of the metabolism-related five genes in mRNA and protein levels. (a) The levels of the five genes in 25 paired cancer and paracancer tissues from Zhongshan Hospital. Paired *t*-test was performed to compare the expression of the target genes. $^{*}P < 0.05$, $^{**}P < 0.01$, $^{***}P < 0.001$. (b) The representative images of five genes in cancer and paracancer tissue. (A color version of this figure is available in the online journal.)

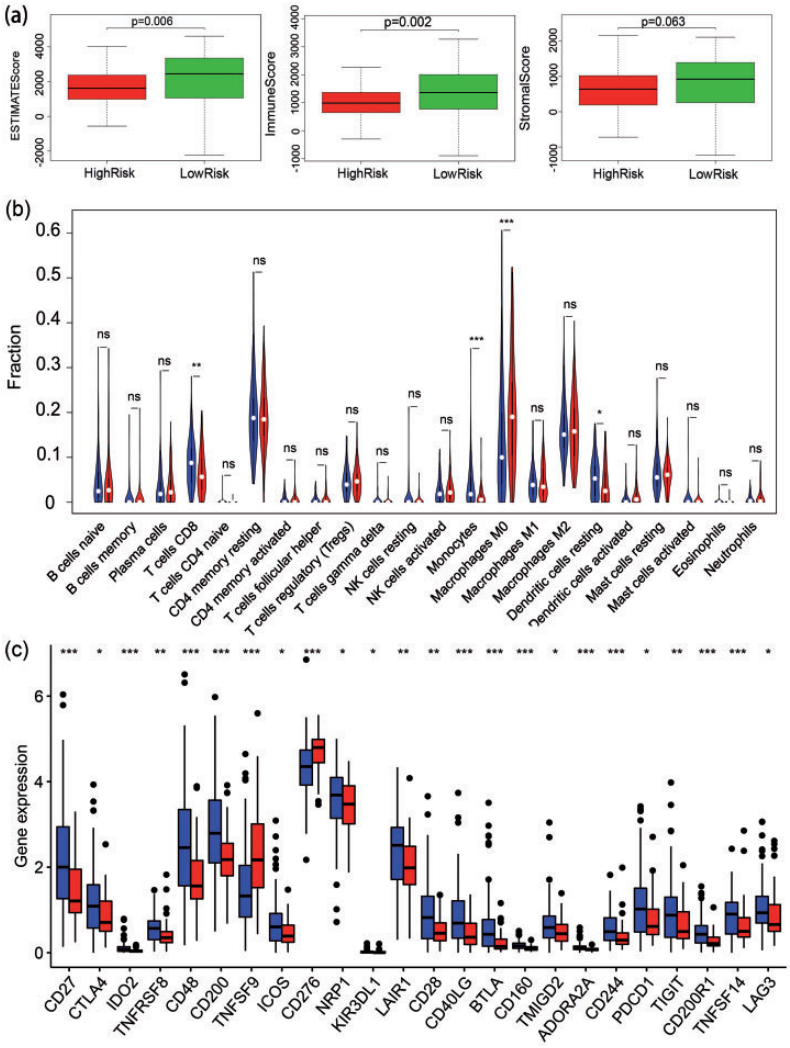

Figure 6. The association between metabolic signature and tumor microenvironment. (a) The comparison of immune scores, stroma scores and ESTIMATE scores. (b) Analysis of differential infiltrating immune cells in TCGA cohort. (c) The differential levels of immunomodulatory molecules between different risk groups. $^{*}P < 0.05$, $^{**}P < 0.01$, $^{***}P < 0.001$. (A color version of this figure is available in the online journal.)

prognostic genes, which may reflect tumor heterogeneity at the molecular level. Recently, several prognostic gene signatures were constructed from different perspectives in PC.[20–22] Compared with previous studies, we constructed the gene signature based on metabolic aberrations of PC, which may shed valuable insights into diagnostic and therapeutic strategies.

Here, we conducted a bioinformatic analysis to identify and validate 109 reliable DEMGs of PC in multiple datasets. Univariate Cox regression analysis discovered 13 DEMGs associated with OS. A novel five-gene signature (B3GNT3, BCAT1, KYNU, LDHA, and TYMS) for prognostic prediction of PC was constructed via Lasso-Cox regression. All five genes were related to poor prognosis, and this metabolic signature was confirmed as an independent prognostic indicator. The prognostic value of signature constructed by the above five genes was assessed in TCGA cohort and further confirmed in GEO cohort.

Then, GSEA revealed that the pathways associated with proliferation and hypoxia were enriched in high-risk group, which further supported that PC cells may reprogram some metabolic pathways to promote survival, proliferation, and differentiation even in a poor nutrient and hypoxic microenvironment.[23] Moreover, it has become evident that the alteration of cell metabolism can regulate the infiltration and function of immune cells.[7] Among them, $CD8^{+}$T cells play extremely important roles in the anti-tumor response. Patients with higher infiltrating $CD8^{+}$T cells in the tumor were prone to have a better prognosis in PC.[24] In our study, the infiltrating $CD8^{+}$ T cells and the degree of immune response seemed to be reduced in the high-risk group. Consistent with our results, two genes (B3GNT3 and LDHA) in our signature have been reported to be associated with immunosuppression. As a glycosyltransferase, B3GNT3 mediated the glycosylation of PD-L1, which participated in immunosuppressive activities. Therefore, B3GNT3 knock-down enhanced the infiltration of $CD8^{+}$T cells and their mediated anti-tumor immunity.[25] LDHA, encoding lactate dehydrogenase A, catalyzes pyruvate to lactate. LDHA overexpression also inhibited the infiltration of $CD8^{+}$T cells and their mediated immune killing.[26,27] Additionally, the expression levels of mostly

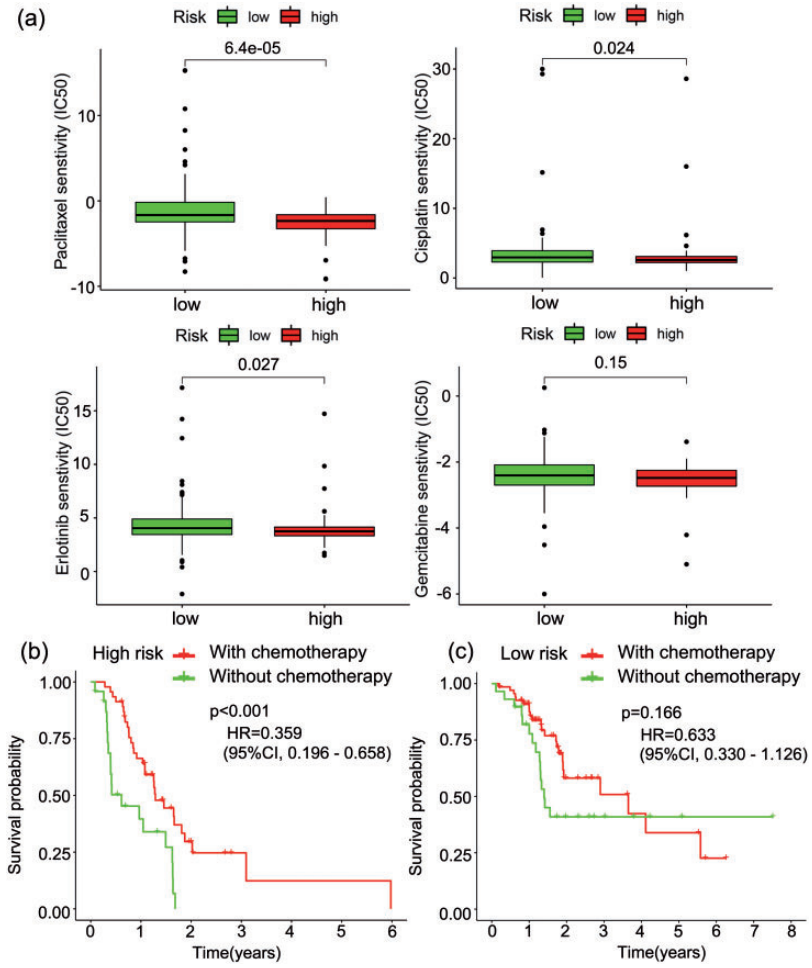

Figure 7. Responses to Chemotherapy in the high- and low-risk groups with PC. (a) Analysis of four common chemotherapeutic responses. (b) The Kaplan-Meier curves for OS in high-risk group with and without chemotherapy. (c) The Kaplan-Meier for OS in low-risk group with and without chemotherapy. OS, overall survival. (A color version of this figure is available in the online journal.)

immunomodulatory molecules were comparatively lower in the high-risk group, further supporting the desertification of tumor immune microenvironment in patients with high risk scores. These results suggested that the patients in the high-risk group might be resistant to the immune checkpoint blockade. This metabolism-related signature might display the changes of the microenvironment to some extent and be valuable to guide proper diagnosis and individualized management.

In addition, it is well known that the malignant biological behavior of PC is accompanied by the acquisition of activated KRAS mutation and loss of TP53 and CDKN2A.[28] KRAS and TP53 mutations, the main driver genes of PC, have been shown to modulate cellar metabolic pathways to maintain pancreatic tumors.[9,29] Consistent with our studies, the rates of KRAS and TP53 mutation were higher in the high-risk group. However, studies about TTN mutation in PC metabolism are scarce and further investigations are needed. Meanwhile, increasing evidence suggested that altered metabolism of PC cells contributed to the chemoresistance[30] and two genes (LDHA and TYMS) in our signature were related to drug resistance as previously reported.[26,31,32] Consistently, the patients with higher risk scores might receive more benefits from chemotherapy.

Taken together, this metabolic signature could assess the prognosis and response to chemotherapy for PC patients. This signature was just calculated by the levels of five selected genes, which was more cost-effective and convenient than whole-genome sequencing. Meanwhile, the nomogram was easy to use for clinicians to accurately assess patients' prognosis. Furthermore, these five genes might be potential molecular targets t, which could be helpful to personalized medicine.

Meanwhile, certain limitations also existed in our work. First, the compositions of both cohorts we used were mostly Whites, Africans, or Latinos. Although our validation cohort was derived from a Chinese population, we only verified the expression of genes in our signature because of the insufficient number of patients. Therefore, extrapolation of our signature to patients from other ethnicities needs further validation. Second, it could not reflect the whole landscape of cancer metabolism merely according to the transcriptomics data. Integration of metabolomics and transcriptomics may be better to discover key metabolic pathways in tumor development and

progression. Third, the development and assessment of the nomogram were conducted via a single database as a result of the inadequate clinicopathological information of other PC databases. The validity and reliability of the formulated nomogram should be further confirmed in the future.

In summary, we established a metabolism-related five-gene signature based on bioinformatics analyses, which was significantly related to PC's progression and immune infiltrations. Additionally, a novel prognostic nomogram integrating the gene signature, age, AJCC_N, and chemotherapy was further established to predict its prognosis, which exhibited a superior ability in predicting OS and may facilitate the potential administration of individual treatment.

AUTHORS' CONTRIBUTIONS

QC, NP, and HY conceived and designed the study. JZ and GZ collected the data. QC analyzed the data. WL and WW supervised for improving research. QC and NP wrote the manuscript. All authors revised the manuscript and approved the final manuscript.

DECLARATION OF CONFLICTING INTERESTS

The author(s) declared no potential conflicts of interest with respect to the research, authorship, and/or publication of this article.

FUNDING

The author(s) disclosed receipt of the following financial support for the research, authorship, and/or publication of this article: This study was supported by Shanghai Sailing Program (21YF1407100), National Natural Science Foundation of China (82103409, 81773068), China Postdoctoral Science Foundation (2021M690037), the National Key R&D Program (2019YFC1315902), and Clinical Science and Technology Innovation Project of the Shanghai ShenKang Hospital Development Centre (SHDC2020CR2017B).

ORCID iD

Wenchuan Wu https://orcid.org/0000-0002-8408-885X

REFERENCES

1. Siegel RL, Miller KD, Fuchs HE, Jemal A. Cancer statistics, 2021. *CA A Cancer J Clin* 2021;**71**:7–33
2. Lai E, Puzzoni M, Ziranu P, Pretta A, Impera V, Mariani S, Liscia N, Soro P, Musio F, Persano M, Donisi C, Tolu S, Balconi F, Pireddu A, Demurtas L, Pusceddu V, Camera S, Sclafani F, Scartozzi M. New therapeutic targets in pancreatic cancer. *Cancer Treat Rev* 2019;**81**:101926
3. Xu JW, Wang L, Cheng YG, Zhang GY, Hu SY, Zhou B, Zhan HX. Immunotherapy for pancreatic cancer: a long and hopeful journey. *Cancer Lett* 2018;**425**:143–51
4. Pu N, Zhao G, Yin H, Li JA, Nuerxiati A, Wang D, Xu X, Kuang T, Jin D, Lou W, Wu W. CD25 and TGF-β blockade based on predictive integrated immune ratio inhibits tumor growth in pancreatic cancer. *J Transl Med* 2018;**16**:294
5. Cairns RA, Harris IS, Mak TW. Regulation of cancer cell metabolism. *Nat Rev Cancer* 2011;**11**:85–95
6. Biancur DE, Kimmelman AC. The plasticity of pancreatic cancer metabolism in tumor progression and therapeutic resistance. *Biochim Biophys Acta Rev Cancer* 2018;**1870**:67–75
7. Riera-Domingo C, Audigé A, Granja S, Cheng WC, Ho PC, Baltazar F, Stockmann C, Mazzone M. Immunity, hypoxia, and metabolism – the ménage à trois of cancer: implications for immunotherapy. *Physiol Rev* 2020;**100**:1–102
8. Chen Q, Pu N, Yin H, Zhang J, Zhao G, Lou W, Wu W. CD73 acts as a prognostic biomarker and promotes progression and immune escape in pancreatic cancer. *J Cell Mol Med* 2020;**24**:8674–86
9. Ying H, Kimmelman AC, Lyssiotis CA, Hua S, Chu GC, Fletcher-Sananikone E, Locasale JW, Son J, Zhang H, Coloff JL, Yan H, Wang W, Chen S, Viale A, Zheng H, Paik JH, Lim C, Guimaraes AR, Martin ES, Chang J, Hezel AF, Perry SR, Hu J, Gan B, Xiao Y, Asara JM, Weissleder R, Wang YA, Chin L, Cantley LC, DePinho RA. Oncogenic Kras maintains pancreatic tumors through regulation of anabolic glucose metabolism. *Cell* 2012;**149**:656–70
10. Hosein AN, Beg MS. Pancreatic cancer metabolism: molecular mechanisms and clinical applications. *Curr Oncol Rep* 2018;**20**:56
11. Ma B, Jiang H, Wen D, Hu J, Han L, Liu W, Xu W, Shi X, Wei W, Liao T, Wang Y, Lu Z, Wang Y, Ji Q. Transcriptome analyses identify a metabolic gene signature indicative of dedifferentiation of papillary thyroid cancer. *J Clin Endocrinol Metab* 2019;**104**:3713–25
12. Szklarczyk D, Franceschini A, Wyder S, Forslund K, Heller D, Huerta-Cepas J, Simonovic M, Roth A, Santos A, Tsafou KP, Kuhn M, Bork P, Jensen LJ, von Mering C. STRING v10: protein-protein interaction networks, integrated over the tree of life. *Nucleic Acids Res* 2015;**43**:D447–52
13. Rhodes DR, Yu J, Shanker K, Deshpande N, Varambally R, Ghosh D, Barrette T, Pandey A, Chinnaiyan AM. ONCOMINE: a cancer microarray database and integrated data-mining platform. *Neoplasia* 2004;**6**:1–6
14. Pu N, Gao S, Yin H, Li JA, Wu W, Fang Y, Zhang L, Rong Y, Xu X, Wang D, Kuang T, Jin D, Yu J, Lou W. Cell-intrinsic PD-1 promotes proliferation in pancreatic cancer by targeting CYR61/CTGF via the hippo pathway. *Cancer Lett* 2019;**460**:42–53
15. Uhlén M, Fagerberg L, Hallström BM, Lindskog C, Oksvold P, Mardinoglu A, Sivertsson Å, Kampf C, Sjöstedt E, Asplund A, Olsson I, Edlund K, Lundberg E, Navani S, Szigyarto CA, Odeberg J, Djureinovic D, Takanen JO, Hober S, Alm T, Edqvist PH, Berling H, Tegel H, Mulder J, Rockberg J, Nilsson P, Schwenk JM, Hamsten M, von Feilitzen K, Forsberg M, Persson L, Johansson F, Zwahlen M, von Heijne G, Nielsen J, Pontén F. Proteomics. Tissue-based map of the human proteome. *Science* 2015;**347**:1260419
16. Subramanian A, Tamayo P, Mootha VK, Mukherjee S, Ebert BL, Gillette MA, Paulovich A, Pomeroy SL, Golub TR, Lander ES, Mesirov JP. Gene set enrichment analysis: a knowledge-based approach for interpreting genome-wide expression profiles. *Proc Natl Acad Sci U S A* 2005;**102**:15545–50
17. Yoshihara K, Shahmoradgoli M, Martínez E, Vegesna R, Kim H, Torres-Garcia W, Treviño V, Shen H, Laird PW, Levine DA, Carter SL, Getz G, Stemke-Hale K, Mills GB, Verhaak RG. Inferring tumour purity and stromal and immune cell admixture from expression data. *Nat Commun* 2013;**4**:2612
18. Newman AM, Liu CL, Green MR, Gentles AJ, Feng W, Xu Y, Hoang CD, Diehn M, Alizadeh AA. Robust enumeration of cell subsets from tissue expression profiles. *Nat Methods* 2015;**12**:453–7
19. Geeleher P, Cox NJ, Huang RS. Clinical drug response can be predicted using baseline gene expression levels and in vitro drug sensitivity in cell lines. *Genome Biol* 2014;**15**:R47
20. Wu M, Li X, Zhang T, Liu Z, Zhao Y. Identification of a Nine-Gene signature and establishment of a prognostic nomogram predicting overall survival of pancreatic cancer. *Front Oncol* 2019;**9**:996
21. Kandimalla R, Tomihara H, Banwait JK, Yamamura K, Singh G, Baba H, Goel A. A 15-Gene immune, stromal, and proliferation gene signature that significantly associates with poor survival in patients with pancreatic ductal adenocarcinoma. *Clin Cancer Res* 2020;**26**:364148
22. Zhou C, Zhao Y, Yin Y, Hu Z, Atyah M, Chen W, Meng Z, Mao H, Zhou Q, Tang W, Wang P, Li Z, Weng J, Bruns C, Popp M, Popp F, Dong Q,

Ren N. A robust 6-mRNA signature for prognosis prediction of pancreatic ductal adenocarcinoma. *Int J Biol Sci* 2019;**15**:228295
23. Qin C, Yang G, Yang J, Ren B, Wang H, Chen G, Zhao F, You L, Wang W, Zhao Y. Metabolism of pancreatic cancer: paving the way to better anticancer strategies. *Mol Cancer* 2020;**19**:50
24. Ino Y, Yamazaki-Itoh R, Shimada K, Iwasaki M, Kosuge T, Kanai Y, Hiraoka N. Immune cell infiltration as an indicator of the immune microenvironment of pancreatic cancer. *Br J Cancer* 2013;**108**:914–23
25. Li CW, Lim SO, Chung EM, Kim YS, Park AH, Yao J, Cha JH, Xia W, Chan LC, Kim T, Chang SS, Lee HH, Chou CK, Liu YL, Yeh HC, Perillo EP, Dunn AK, Kuo CW, Khoo KH, Hsu JL, Wu Y, Hsu JM, Yamaguchi H, Huang TH, Sahin AA, Hortobagyi GN, Yoo SS, Hung MC. Eradication of triple-negative breast cancer cells by targeting glycosylated PD-L1. *Cancer cell*. 2018;**33**:187–201.e10
26. Feng Y, Xiong Y, Qiao T, Li X, Jia L, Han Y. Lactate dehydrogenase A: a key player in carcinogenesis and potential target in cancer therapy. *Cancer Med* 2018;**7**:6124–36
27. Brand A, Singer K, Koehl GE, Kolitzus M, Schoenhammer G, Thiel A, Matos C, Bruss C, Klobuch S, Peter K, Kastenberger M, Bogdan C, Schleicher U, Mackensen A, Ullrich E, Fichtner-Feigl S, Kesselring R, Mack M, Ritter U, Schmid M, Blank C, Dettmer K, Oefner PJ, Hoffmann P, Walenta S, Geissler EK, Pouyssegur J, Villunger A, Steven A, Seliger B, Schreml S, Haferkamp S, Kohl E, Karrer S, Berneburg M, Herr W, Mueller-Klieser W, Renner K, Kreutz M. LDHA-associated lactic acid production blunts tumor immunosurveillance by T and NK cells. *Cell Metab* 2016;**24**:657–71
28. Waddell N, Pajic M, Patch AM, Chang DK, Kassahn KS, Bailey P, Johns AL, Miller D, Nones K, Quek K, Quinn MC, Robertson AJ, Fadlullah MZ, Bruxner TJ, Christ AN, Harliwong I, Idrisoglu S, Manning S, Nourse C, Nourbakhsh E, Wani S, Wilson PJ, Markham E, Cloonan N, Anderson MJ, Fink JL, Holmes O, Kazakoff SH, Leonard C, Newell F, Poudel B, Song S, Taylor D, Waddell N, Wood S, Xu Q, Wu J, Pinese M, Cowley MJ, Lee HC, Jones MD, Nagrial AM, Humphris J, Chantrill LA, Chin V, Steinmann AM, Mawson A, Humphrey ES, Colvin EK, Chou A, Scarlett CJ, Pinho AV, Giry-Laterriere M, Rooman I, Samra JS, Kench JG, Pettitt JA, Merrett ND, Toon C, Epari K, Nguyen NQ, Barbour A, Zeps N, Jamieson NB, Graham JS, Niclou SP, Bjerkvig R, Grützmann R, Aust D, Hruban RH, Maitra A, Iacobuzio-Donahue CA, Wolfgang CL, Morgan RA, Lawlor RT, Corbo V, Bassi C, Falconi M, Zamboni G, Tortora G, Tempero MA, Gill AJ, Eshleman JR, Pilarsky C, Scarpa A, Musgrove EA, Pearson JV, Biankin AV, Grimmond SM. Whole genomes redefine the mutational landscape of pancreatic cancer. *Nature* 2015;**518**:495–501
29. Morris JPt Yashinskie JJ, Koche R, Chandwani R, Tian S, Chen CC, Baslan T, Marinkovic ZS, Sánchez-Rivera FJ, Leach SD, Carmona-Fontaine C, Thompson CB, Finley LWS, Lowe SW. α-Ketoglutarate links p53 to cell fate during tumour suppression. *Nature* 2019;**573**:595–9
30. Grasso C, Jansen G, Giovannetti E. Drug resistance in pancreatic cancer: impact of altered energy metabolism. *Crit Rev Oncol Hematol* 2017;**114**:13952
31. Johnston PG, Drake JC, Trepel J, Allegra CJ. Immunological quantitation of thymidylate synthase using the monoclonal antibody TS 106 in 5-fluorouracil-sensitive and -resistant human cancer cell lines. *Cancer Res* 1992;**52**:4306–12
32. Johnston PG, Lenz HJ, Leichman CG, Danenberg KD, Allegra CJ, Danenberg PV, Leichman L. Thymidylate synthase gene and protein expression correlate and are associated with response to 5-fluorouracil in human colorectal and gastric tumors. *Cancer Res* 1995;**55**:1407–12

(Received July 2, 2021, Accepted September 8, 2021)